RSC Advances

ROYAL SOCIETY OF CHEMISTRY

www.rsc.org/advances

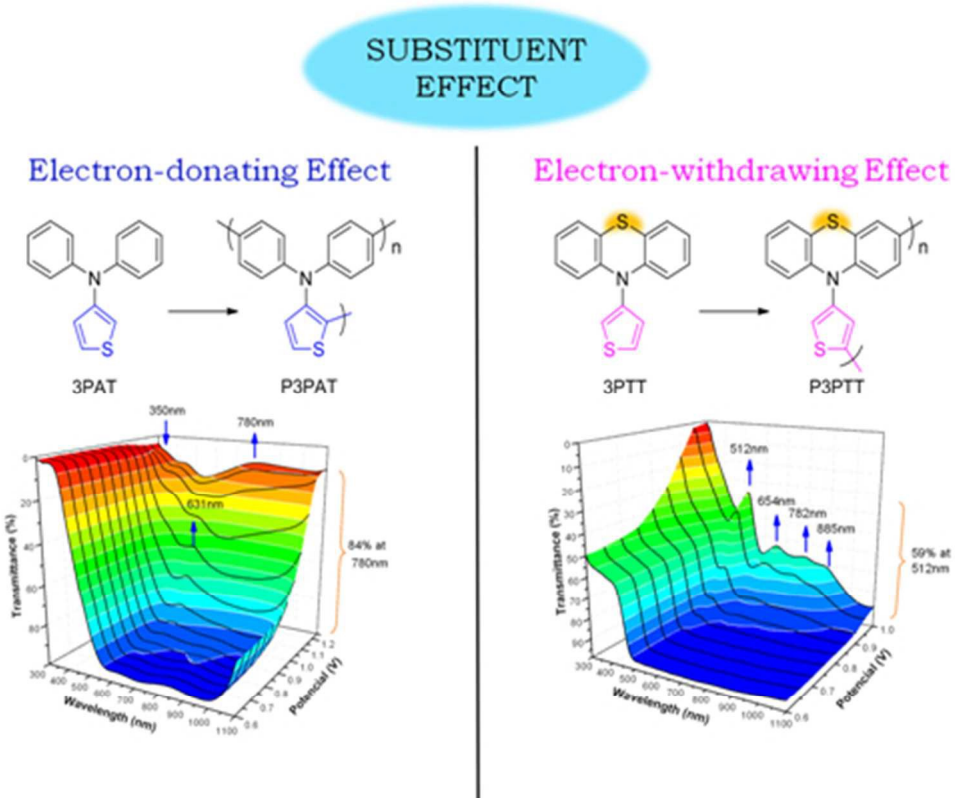

42x34mm (300 x 300 DPI)

The sole difference in chemical structure plays a role in inflecting reactivity, probably through altering electron cloud density.

Cite this: DOI: 10.1039/c0xx00000x

www.rsc.org/xxxxxx

ARTICLE TYPE

Synthesis, Structures, and Electrochromic Behaviors of Poly(triarylamine)s based on 3-substituted Thiophene Derivatives

Jinrui Lin [a] and Xiuyuan Ni *[a]

Two triarylamine-based polymers were synthesized by the oxidative coupling reactions from 3-(N, N-diphenylamino) thiophene (3PAT) and 3-(10H-phenothiazin-10-yl) thiophene (3PTT) monomers, respectively. Distinguished from 3PAT, 3PTT has an additional sulfur atom between the two benzene rings. By using NMR spectroscopy and triarylamine control, the structures of the synthesized polymers were resolved with the aim to reveal the substitution effect. The results present that the substituent plays an important role in the chain propagation. Moreover, the triarylamine-based polymers were investigated about their solubility, thermal stability and electrochemical properties. To evaluate the electrochromism of the two different polymers, we have measured the spectroelectrochemical and electrochromic switching properties from the solution-cast films.

Introduction

Distinguished from the conventional π conjugated polymers, triarylamine-based polymers have the propeller-like unit comprising a nitrogen center in connection with three electron-rich aromatic rings. The good hole-transporting ability is one of the remarkable properties possessed by the triarylamine-based polymers and thus has attracted a great deal of attention.[1] The polymer structure that is featured by the electroactive nitrogen center, non-plane geometry and conjugated aromatic rings affords the capability of hole injection and transfer. Their aromatic structures also provide high thermal stability. However, it is difficult for the triarylamine homopolymers to dissolve in solvents and thus, these polymers were usually processed by means of vapor depositing instead of the easy-to-perform solution techniques.[2] Having potential to gain large–area devices and to avoid a thermal degradation in the vapor deposition, soluble triarylamine-based polymers are preferred for fabricating electronic devices.[3] Triphenylamine-based polymers are used as the hole-transporting layer in various kinds of devices such as light emitting diodes and solar cells.[4] The organic solar cells, which employ the triarylamine-based polymers as the hole-transporting layer, usually show good conversion efficiency and stability due to avoiding hole traps and corrosion on indium-tin oxide (ITO) electrodes.[5,6] Moreover, the triarylamine-based polymers are noticed for their electrochromic performance.[7] The nitrogen atoms serve as the reversible redox center at a low applied potential. In contrast to small molecular compounds, the triarylamine-based polymers usually have stable morphologies due to prevention of crystallization and exfoliation. Lots of triarylamine-based polymers with good electrochromic properties were synthesized through introducing multiple redox-active amino centers to the monomers, changing electron-rich and electron-poor character in the repeat units or copolymerizing with different monomers randomly.[8]

The electrochemical polymerization has been broadly used to deposit triarylamine-based polymers on the electrodes. For instances, Ramírez et al.[9] have used this method to synthesize the polymers from new tetraphenyl-4, 4'-diaminodiphenylmethane derivatives. Yang et al.[10] have reported an electrochemical polymerization of triphenylamine-containing indoline dye on the TiO_2 photoelectrodes. Moreover, a variety of synthetic strategies has been developed for pursuing new structures which include the polymers easy to dissolve in solvents. By using Friedel-Crafts type condensation,[11] poly (p-methylenetriphenylamine) was synthesized to have the backbones comprising dendritic, linear and terminal units. Manuel et al.[12] have synthesized a series of styrene derived triarylamines through Ullmann reaction[13]. The molecular weights, polydispersities and glass transition temperatures were controlled by altering side groups. Lin et al.[14] have synthesized polytriphenylamines via oxidative coupling polymerization and observed that the monomers which contained the electron-withdrawing substituent had the molecular weight hundred times more than that of containing electron-donating substituent. Moreover, the method of Suzuki polycondensation[15] was applied to synthesize triarylamine-based hyperbranched polymers of different band gaps, in which the difunctional core molecules and flexible alkyl chains were introduced for the purpose of dissolving polymers in organic solvents.

At the present, the triarylamine-based polymers were synthesized almost from triphenylamine derivatives. In the polymerizations, the benzene ring in those monomers performed the reacting site only at the para-position. Recently, Keans et al.[16] have reported the electrochemical polymerization of tris (4-(thiophen-2-yl) phenyl) amine, which is one of thiophene-containing triarylamine. In that case, either 4-position or 5-position in the thiophene ring can take part in the chain propagation. By introducing block group to 4-position in the thiophene ring, the synthesized polymer showed high electric capacity, which was correlated to the change in the structural regularity. In the conventional thiophene-containing triarylamines, the thiophene ring is connected to the nitrogen atom center via 2-position, while 5-position can take part in chain propagation. It is noted that as for thiophene-3-yl arylamine, the polymerization route remains unclear as yet. Knowledge of the reactivity of the monomers allows controlling their polymerization.

In this paper, we report the oxidative coupling polymerization of 3-(N, N-diphenylamino) thiophene (3PAT) and 3-(10H-phenothiazin-10-yl) thiophene (3PTT). The synthesis aims to provide new poly(triarylamine)s as functional materials for the use in fabricating electronic devices. The obtained two polymers, P3PAT and P3PTT, have good solubility in the conventional organic solvents. Films are prepared from the polymer solutions and are measured here with respect to electrochromism. In this study, 3PAT and 3PTT are chosen as the model compounds for exploring how the substituent affects the monomer reactivity. The polymer products are analyzed by using nuclear magnetic resonance spectroscopy and cyclic voltammetry. The results prove 3PAT and 3PTT to show sole but different reaction site in the thiophene rings. It is obtained that both of P3PAT and P3PTT display reversible electrochromic behaviors with low potentials, and they exhibit high optical contrast at different wavelengths.

Experimental Section

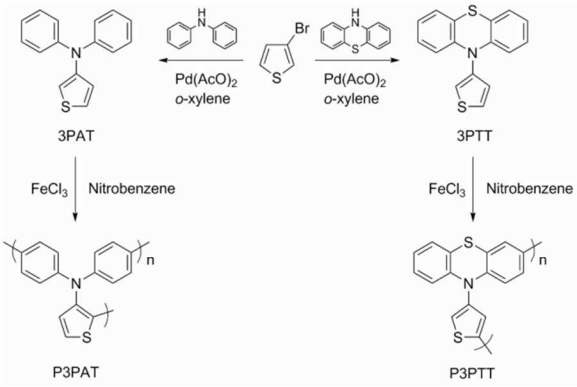

Scheme 1 The reaction routes to synthesize 3-(N, N-diphenylamino) thiophene (3PAT) and 3-(10H-phenothiazin-10-yl) thiophene (3PTT) from 3-bromothiophene and the oxidation polymerization of 3PAT and 3PTT.

Materials

Sodium tert-butoxide, tri-tert-butylphosphine, palladium (II) Acetate, diphenylamine, phenothiazine and o-xylene were purchased from Aladdin. 3-bromothiophene was purchased from J&K. Diphenylamine and phenothiazin were purified by recrystallization from hexane. Tetrabutylammonium hexafluorophosphate was recrystallized twice from ethyl acetate and then dried *in vacuo* prior to use. Chloroform, *o*-xylene and nitrobenzene were distilled over calcium hydride. All other reagent grade materials and solvents were purchased from Sinopharm Chemical Reagent Co., Ltd and used without further purification.

Monomer Synthesis

3-(N, N-diphenylamino) thiophene (3PAT). 3-(N, N-diphenylamino) thiophene was synthesized by palladium acetate-catalyzed coupling of 3-bromothiophene and diphenylamine,[17] as illustrated by the reaction sequence in Scheme 1. 3-bromothiophene (0.34g, 2 mmol), diphenylamine (0.776 g, 2 mmol), $Pd(OAc)_2$ (4.49 mg, 0.02 mmol) and sodium tert-butoxide (0.211 g, 2.4 mmol) were weighted directly into a three-necked flask. Then, a solution of tri-tert-butylphosphine in toluene (1 M, 0.06 mL) and 10 mL of anhydrous o-xylene were added. The mixture was refluxed for 3 h under an argon atmosphere. The hot reaction mixture was poured into pentane (10 mL), filtered to remove insoluble solids, and concentrated *in vacuo* to give a yellow powder. The crude product was purified by chromatography using hexane/ether (19: 1) as the eluent. 0.36 g (1.43 mmol, yield 72%) of 3-(N, N-diphenylamino) thiophene was obtained as pure white solid. Melting point: 95-96 ℃. FTIR (see figure S1, KBr pellet, cm^{-1}): 1487(C=C symmetrical stretching vibration), 1384 (C=C asymmetrical stretching vibration), 1528(C-C stretching vibration), 1151(C-H bending vibration), 1309(C-N stretching vibration with aromatic conjugation). ^1H NMR (500 MHz, $CDCl_3$, ppm): δ=7.21-7.25 (m, 5H), 7.085(d, J = 7.5 Hz, 4H), 6.99 (t, J = 7.5 Hz, 2H), 6.868 (d, J =5 Hz, 1H), 6.65 (s, 1H). The ^1H NMR spectrum of 3PAT is illustrated in Figure S3a. $^{13}C\{^1H\}$ NMR(126MHz, $CDCl_3$, ppm) δ=147.84, 146.56, 129.13, 124.90, , 123.10, 122.961, 112.86; EIMS(m/z): 251.2 (M^+). Anal. Calcd (%) for $C_{16}H_{13}NS$ (251.37): C, 76.44%; H, 5.22%; N, 5.57%. Found: C, 76.50%; H, 5.20%; N, 5.54%.

3-(10H-phenothiazin-10-yl) thiophene (3PTT). 3-(10H-phenothiazin-10-yl) thiophene was synthesized by palladium acetate-catalyzed coupling reaction. 3-bromothiophene (0.34g, 2 mmol), phenothiazine (0.914g, 2 mmol), $Pd(OAc)_2$ (4.49 mg, 0.02 mmol) and sodium tert-butoxide (0.211 g, 2.4 mmol) were added into a three-necked flask. Then, a solution of tri-tert-butylphosphine in toluene (1 M, 0.06 mL) and 10 mL of anhydrous *o*-xylene were added. The mixture was refluxed at 145 ℃ for 3 h under an argon atmosphere. The reaction mixture was poured into pentane (10 mL), filtered, and concentrated *in vacuo* to give a yellow powder. The crude product was purified by chromatography using hexane/ether (19 : 1) as the eluent. 0.47 g (1.66 mmol, yield 83%) of 3-(10H-phenothiazin-10-yl) thiophene was obtained as pure white solid. Melting point: 103-104 ℃. FTIR (see figure S1, KBr pellet, cm^{-1}): 1485(C=C symmetrical stretching vibration), 1373 (C=C asymmetrical stretching vibration), 1526 (C-C stretching vibration), 1155(C-H bending vibration), 1307(C-N stretching vibration with aromatic conjugation). ^1H NMR (500 MHz, $CDCl_3$, ppm): δ=7.57 (dd, J = 4.5, 3.0 Hz 1H), 7.38(d, J = 1.5 Hz, 1H), 7.15 (d, J = 5 Hz, 1H), 7.06 (d, J =7.5 Hz, 2H), 6.93 (t, J = 6 Hz, 2H), 6.92 (t, J = 7.5 Hz, 2H),6.39 (d, J = 4 Hz, 2H). ^1H NMR spectrum of 3PTT is illustrated in Figure S3b. $^{13}C\{^1H\}$ NMR(126MHz, $CDCl_3$, ppm): δ=144.28, 139.40, 128.17, 127.02, 126.78, 123.79, 122.72, 120.62, 116.05; EIMS(m/z): 281.1 (M^+). Anal. Calcd (%) for $C_{16}H_{11}NS_2$ (281.42): C, 68.28%; H, 3.95%; N, 4.98%. Found: C, 68.25%; H, 3.95%; N, 4.94%.

Polymer Synthesis.

Poly(3-(N, N-diphenylamino) thiophene) (P3PAT). Poly(3-(N, N-diphenylamino) thiophene) was synthesized by chemical oxidative coupling reaction. Nitrobenzene (10 ml) and $FeCl_3$ (1.944 g, 12 mmol) were added into a three-necked flask containing 3PAT (1.255 g, 5 mmol) under argon atmosphere. The solution was stirred for 12 h at room temperature, and then poured into methanol to deposit product. The crude polymer powders were collected and washed with aqueous ammonium hydroxide, repurified from chloroform into methanol twice and then dried *in vacuo* at 50 ℃ for 12 h. FTIR (see figure S1, KBr

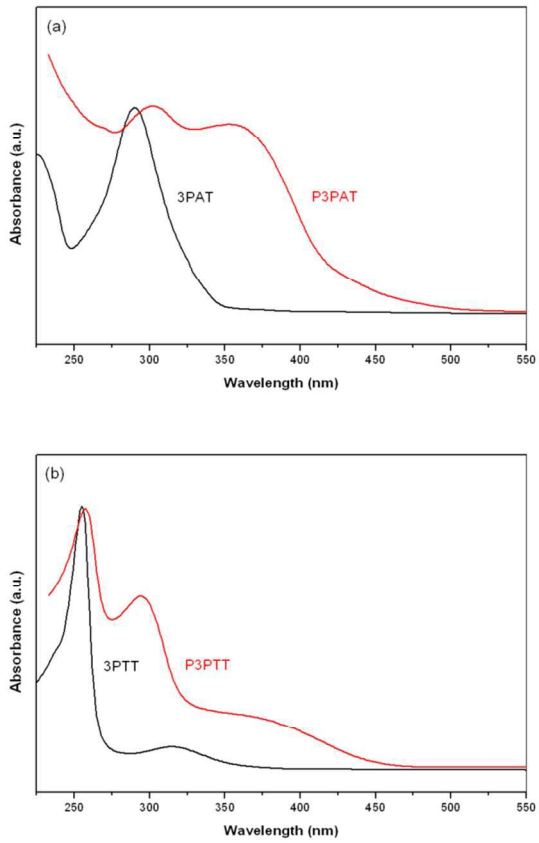

Fig. 1 UV-vis absorbance spectra measured from (a) 3PAT, P3PAT and (b) 3PTT, P3PTT in CH_2Cl_2 solution.

pellet, cm^{-1}): 1492(C=C symmetrical stretching vibration), 1383 (C=C asymmetrical stretching vibration), 1533(C-C stretching vibration), 1155(C-H bending vibration), 1311(C-N stretching vibration with aromatic conjugation). Anal. Calcd (%) for $C_{16}H_{10}NS$ (248.34): C, 77.38%; H, 4.07%; N, 5.64%. Found: C, 74.55%; H, 5.12%; N, 5.48%.

Poly(3-(10H-phenothiazin-10-yl) thiophene) (P3PTT). Poly(3-(10H-phenothiazin-10-yl) thiophene) was prepared by chemical oxidative coupling reaction using $FeCl_3$ as an oxidant. Nitrobenzene (10 ml) and $FeCl_3$ (1.539 g, 9.5 mmol) were added into a three-necked flask containing 3PTT (0.728 g, 2.5 mmol) under argon atmosphere. The solution was stirred for 20 h at room temperature and poured slowly into methanol giving rise to a green precipitate that collected by filtration, washed with aqueous ammonium hydroxide, repurified from chloroform into methanol twice and then dried *in vacuo* at 50 ℃ for 12 h. FTIR (see figure S1, KBr pellet, cm^{-1}): 1492(C=C symmetrical stretching vibration), 1374 (C=C asymmetrical stretching vibration), 1532(C-C stretching vibration), 1159(C-H bending vibration), 1309(C-N stretching vibration with aromatic conjugation). Anal. Calcd (%) for $C_{16}H_9NS_2$ (278.60): C, 68.97%; H, 3.26%; N, 5.03%. Found: C, 69.01%; H, 3.65%; N, 5.31%.

Measurements.

Fourier transform infrared (FTIR) spectra were recorded using a Nicolet 6700 spectrometer. The melting points were measured by using a TA Q2000 Differential Scanning Calorimeter (DSC) at a heating rate of 1 ℃/min. UV-vis spectra were recorded on a Perkin-Elmer Lamb 35 Spectrophotometer. Elemental analyses of carbon, hydrogen and oxygen were carried out with an Elementar Vario EL cube elemental Analyzer. The molecular weight of P3PAT and P3PTT were determined using gel-permeation chromatography (GPC) (Agilent 1260/Wyatt) at 25 ℃, using tetrahydrofuran (THF) as eluent and polystyrenes as standards. ^1H and ^{13}C NMR spectra were recorded on a Bruker AV-500 FT-NMR system with deuterated chloroform as the solvent. Thermogravimetric analysis (TGA) was carried out using a PerkinElmer Pyris 1 TGA at a heating rate of 20 ℃·min^{-1} under nitrogen or air at a flow rate of 40 cm^3/min. Cyclic voltammetry was recorded on a CHI660 electrochemical workstation. The experiments were based on a conventional three-electrode system composed of Glassy carbon electrode as a working electrode, a platinum wire as an auxiliary electrode and a Ag/AgCl (saturated KCl) as reference electrode. The spectroelectrochemistry of polymer films were measured in an electrolytic cell which was composed of a platinum wire auxiliary electrode and an Ag/AgCl reference electrode.

Results and Discussion

The polymer structures

Table 1 Molecular weight and thermo properties of the polymers

Polymer code	Yield(%)	Mw[a]	PDI[b]	Solubility (g/ml)	T_d at 10% Weight loss(℃)[c] N_2	T_d at 10% Weight loss(℃)[c] Air	Carbonized residue (wt %)[d]
P3PAT	48	4700	1.38	0.5	495	456	75
P3PTT	85	3900	1.37	0.03	557	554	54

[a] Weight-average molecular weights relative to polystyrene standards in THF by GPC. [b] PDI =Mw/Mn. [c] Decomposition temperature, recorded via TGA at a heating rate of 20 ℃/min and a gas-flow rate of 40 cm^3/min. [d] Solubility, measured in chloroform. [e] Residual weight percentage at 800 ℃in nitrogen.

As shown by the characterization results in Table 1, P3PAT and P3PTT have a weigh- average molecular weight (M_w) of 4730 and 3920, respectively. Each of them shows considerable narrow polydispersity (PDI) around 1.37. The two polymers are highly soluble in the conventional organic solvents, admitting the use of solution casting technique. In particular, P3PAT can be more easily dissolved in chloroform, the concentration as high as 500 mg·ml^{-1} at room temperature. By analyzing thermogravimetric data, we obtain that both P3PAT and P3PTT hold remarkable stability to thermal oxidization. The temperatures at the weight-loss of 10% are 456℃ for P3PAT and 554℃ for P3PTT in air atmosphere, respectively (Table 1). The amount of the carbonized residue in nitrogen is 75% for P3PAT and 54% for P3PTT at 800 ℃. The TGA curve of polymer is given in the Supporting Information (Figure S2). The high char yields are ascribed to the aromatic nature of the synthesized two polymers.

Figure 1 shows the UV-vis spectra which are measured from the monomers and polymers in dichloromethane, respectively.

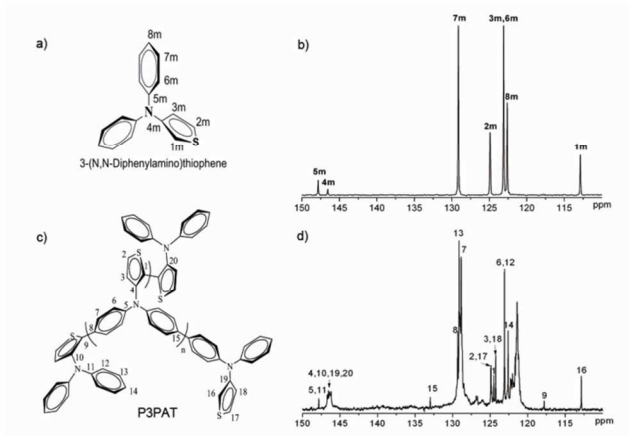

Fig. 2 (a): The structural diagram of 3PAT; (b): The ^{13}C-NMR spectrum of 3PAT; (c): The structural diagram of P3PAT; (d) The ^{13}C-NMR spectrum of P3PAT.

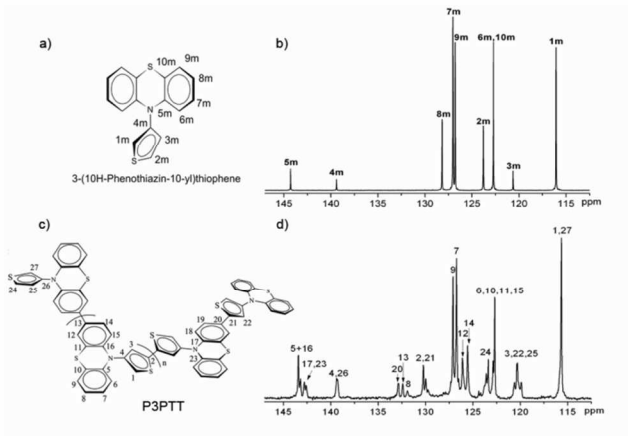

Fig.3 (a): The structural diagram of 3PTT; (b): The ^{13}C-NMR spectrum of 3PTT; (c): The structural diagram of P3PTT; (d) The ^{13}C-NMR spectrum of P3PTT.

The 3PAT monomer shows the absorption peak at 290 nm, which originates from the π-π* transition of the conjugated moieties. It is observed that P3PAT shows two absorption peaks at 302 nm and 352 nm, which are attributed to the π-conjugated chain. The 3PTT monomer has two characteristic absorption bands centered at 254 nm and 314 nm, respectively. The two bands are assigned to the strong π-π* transition and weak intramolecular charge-transfer interaction, respectively.[18] In the UV-vis spectrum of P3PTT, two main absorption peaks at 258 nm and 294 nm and a shoulder peak at 372 nm. Band gaps for P3PAT and P3PTT were estimated from the low-energy band edges of the UV-vis absorption spectra in the film state.[19] Optical band gaps of P3PAT and P3PTT are estimated to be 2.51 eV and 2.63 eV, respectively.

Table 2 ^{13}C NMR chemical shifts of Ph_3N derivatives as reference

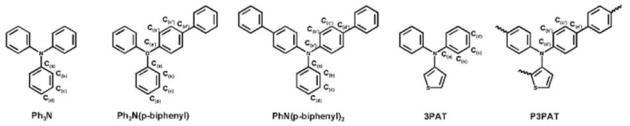

	carbon on C_6H_5- rings		carbon on substituted rings		Δδ(ppm)	Δδ(ppm)
	$C_{(c)}$	$C_{(d)}$	$C_{(c')}$	$C_{(d')}$	$\delta_{(c')}$- $\delta_{(c)}$	$\delta_{(d')}$- $\delta_{(d)}$
Ph_3N[a]	129.2	122.5				
Ph_2N(p-biphenyl)[b]	129.2	122.9	127.7	135.1	-1.5	12.2
PhN(p-biphenyl)$_2$[c]	129.3	123.1	127.8	135.4	-1.4	12.3
3PAT	129.1	122.6				
P3PAT	129.1	122.6	128.8	133.0	-0.3	10.4

[a] ^{13}C chemical shifts from reference 20. [b] ^{13}C chemical shifts from reference 21. [c] ^{13}C chemical shifts from reference 22.

For assisting ^{13}C NMR identification of the fine structures in our polymers, Ph_3N, Ph_2N(p-biphenyl) and PhN(p-biphenyl)$_2$ are adopted as references. Their molecular formula and characteristic chemical shifts are summarized in Table 2. Ph_3N[20] has a quartet of resonance signals at 147.6 ppm, 124.0 ppm, 129.2 ppm and 122.5 ppm. They are assigned to $C_{(a)}$, $C_{(b)}$, $C_{(c)}$ and $C_{(d)}$ atoms, respectively. Ph_2N(p-biphenyl)[21] has an octet of resonance signals: $C_{(a)}$, $C_{(b)}$, $C_{(c)}$ and $C_{(d)}$ atoms retain at the same chemical shifts as Ph_3N; The resonance signals of $C_{(a')}$, $C_{(b')}$, $C_{(c')}$ and $C_{(d')}$ appear at 147.1 ppm, 124.0 ppm, 127.7 ppm and 135.1 ppm, respectively. It is apparent that the phenyl substitution brings about a downfield shift as much as 12.2 ppm to the substitute $C_{(d')}$ and an upfield shift of 1.5 ppm to the adjacent $C_{(c')}$ atom, while $C_{(a')}$ and $C_{(b')}$ are less influenced. In PhN(p-biphenyl)$_2$,[22] the signal of the substituted $C_{(d')}$ downfield shifts by 12.9 ppm, and signals of $C_{(c')}$ upfield shifts by 1.4 ppm, as indicated by the data in Table 2. The spectral properties of these Ph_3N derivatives demonstrate that the phenyl substitution can bring about the downfield shift of more than 10 ppm to the ipso carbon atoms and lead to an upfield shift around 1ppm for the ortho carbon atoms.

Figure 2 shows the ^{13}C NMR spectra of 3PAT and P3PAT. The ^{13}C NMR spectrum of the polymer is identified by taking account of the spectrum of 3PAT and the phenyl substituent effect on the upfield-downfield shift relationships, which has played in the Ph_3N derivatives as above. The assignments are presented in Figure 2d. The results reveal that 3PAT is polymerized by C8m and C1m being covalently linked, as depicted in Figure 2c. With approximate chemical shift as C8m in 3PAT, the signal at 122.5 ppm measured for P3PAT is assigned to C14 on the terminals of chain. The signal of C15, phenyl-substituted carbon atoms, downfield shifts obviously by 10.37 ppm as compared to C8m. Due to thienyl substituent, a downfield shift of 6.68 ppm is observed for C8 than C8m. Affected by the thienyl substituent, C7 as an ortho carbon atom shows an upfield shift compared to C7m. In addition, the remnant, carbon atoms in the para position have signals in the range from 120.6 ppm to 122.4 ppm, depending on the number of substituent.[11] As compared with C1m, C1 in P3PAT downfield shifts by 11.71 ppm due to thienyl substituent, and the signal of C9 downfield shifts by 4.97 ppm due to phenyl substituent. Since C1, C8 and C15 bear the propagation reaction, the resulted polymers have a branched structure as shown in Figure 2.

In Figure 3, the ^{13}C NMR spectrum of P3PTT is shown together with the ^{13}C NMR spectra of 3PTT. Analyzing ^{13}C NMR spectral data reveals that 3PTT is polymerized with C8m and C2m being covalently bound. The signal assignments are

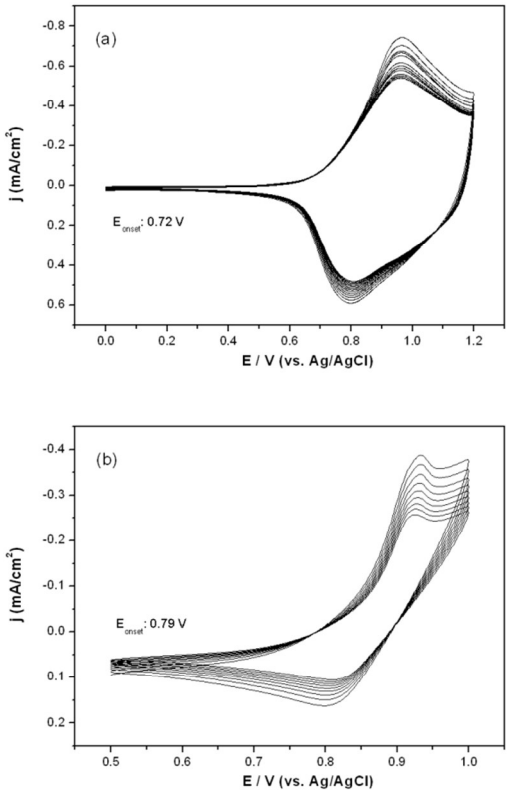

Fig.4 The cyclic voltammograms measured from (a) P3PAT and (b) P3PTT on an ITO glass in 0.1 M n-Bu_4NPF_6/CH_3CN solution at a scan rate of 100 mV/s.

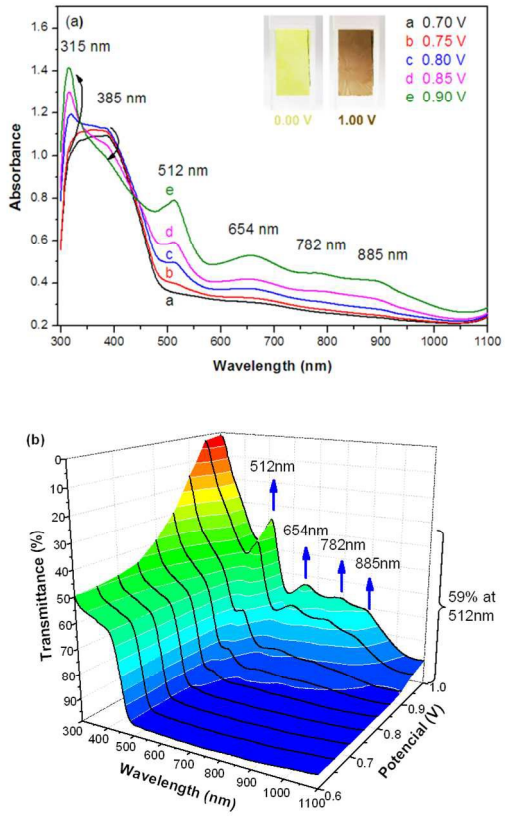

Fig. 5 The spectroelectrochemistry curves measured from the P3PTT film at varied applied potentials. (a): The absorbance spectra of the P3PTT film; (b) The 3D electrochromic properties of the P3PTT film. The electrolyte was 0.1 M n-Bu_4NPF_6 in CH_3CN. The applied voltages were from 0.60 V to 1.00 V in a stepwise fashion with a step size of 0.05 V.

presented in Figure 3d. In the ^{13}C NMR spectrum of 3PTT monomer, the signal at 128.20 ppm is attributed to C8m (Figure 3b). It is found in Figure 3d that this signal fades away from the P3PTT spectrum and so, the phenothiazine moieties have been linked into the chain through C8m. Also in the P3PTT spectrum, the new signals at 132.39 ppm and 132.87 ppm are assigned to C13 and C20, respectively. The two carbons bear the 10H-phenothiazine-3-yl and thienyl substituent, respectively (Figure 3c). In response to these substitutions, the adjacent C12 and C14 upfield shifted. As seen, an upfield shift of about 1 ppm consistently occurs between C12 and C9m and between C14 and C7m. The signals at 143.2 ppm, 142.8 ppm and 142.6 ppm are assigned to C16, C17 and C18, respectively. Their upfield shifts in comparison with C5m are related to the substitution induced change in the electron cloud density of phenothiazine.[23] As for C2m of 3PTT, the carbon atoms are substituted in the chain by either 10H-phenothiazine-3-yl or thienyl (Figure 3c). As compared to C2m, the resonance signals of the substituted C2 and C21 downfield shift by 6.5 ppm and 6.2 ppm, respectively.

As indicated by the above NMR assignments, both of the two benzene rings at 3PAT can take part in the reaction of chain propagation, whereas one of the two benzene rings at 3PTT is bound leading to a linear polymer (Figure 3c). Moreover, during the polymerization the thiophene ring at 3PAT exhibit distinct reactive sites from the thiophene ring at 3PTT. As measured by the NMR spectroscopy, the reactions in the thiophene rings occur at C1 atoms for 3PAT and C2 atoms for 3PTT. The result can be attributed to electron-withdrawing effect and electron-donating effects of 10H-phenothiazine-3-yl group and diphenylamino group, respectively. As compared to the diphenylamino group, the electrons of the nitrogen atom prefer to localize within the phenothiazine ring, making the 10H-phenothiazine-3-yl group an electron withdrawing group. Distinguished from 3PAT, 3PTT has the chemical structure with a sulfur atom between two benzene rings. Our results reveal that the sole difference in chemical structure plays a role in inflecting reactivity, probably through altering electron cloud density.

Electrochemical and Electrochromic properties

Table 3 Electrochemical properties of P3PAT and P3PTT

Code	E_{onset}[a](V)	HOMO(eV)[b]	LUMO(eV)[c]	Eg_{opt}[d]
P3PAT	0.72	-4.96	-2.45	2.51
P3PTT	0.79	-5.13	-2.50	2.63

[a] Onset potentials (V vs. Ag/AgCl) in CH_3CN containing 0.1 M Tetrabutylammonium hexafluorophosphate (n-Bu_4NPF_6). [b] The HOMO energy levels were calculated from cyclic voltammetry and were referenced to ferrocene (4.8 eV). E_{HOMO}= -[E_{ox}- $E_{(Fc/Fc+)}$ + 4.8] Ev; $E_{(Fc/Fc+)}$ =0.46. [c] E_{LUMO}=Eg + E_{HOMO}. [d] Band gaps obtained from onset absorption (λ_{onset}): Eg=1240/λ_{onset}.

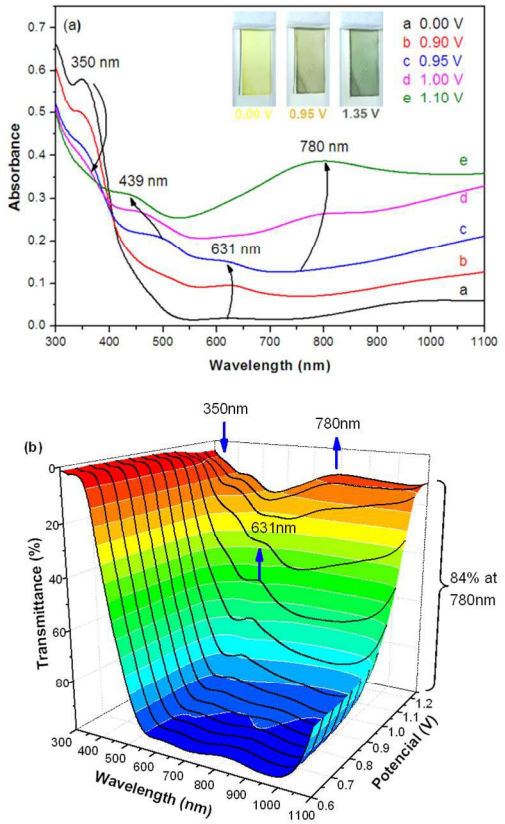

Fig. 6 The spectroelectrochemistry curves measured from the P3PAT film at varied applied potentials. (a): The absorbance spectra of the P3PAT film; (b) The 3D electrochromic properties of the P3PAT film. The electrolyte was 0.1 M n-Bu_4NPF_6 in CH_3CN. The applied voltages were from 0.60 V to 1.25 V in a stepwise fashion with a step size of 0.05 V.

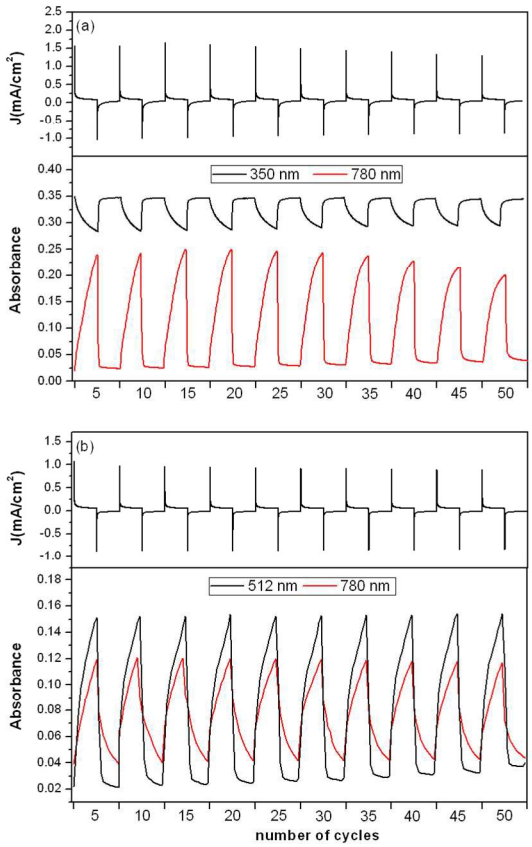

Fig. 7 Electrochromic switching of (a) the P3PAT film with the applied voltages between 0 and 1.25 V and (b) the P3PTT film with the applied voltages from 0 and 1.00 V. The electrolyte was 0.1 M n-Bu_4NPF_6 in CH_3CN.

According to the absorption onset in the UV-vis curves as shown in Figure 1, the band gap (E_g) of the polymers are calculated and listed in Table 3. By using cyclic voltammetry in n-Bu_4NPF_6/MeCN electrolyte, the polymer films, which are prepared from the chloroform solution, are measured for the electrochemical properties. As indicated by the redox curves in Figure 4, P3PAT and P3PTT exhibit typically reversible progress with onset oxidation potential of 0.72 V for P3PAT and 0.79 V for P3PTT. Therefore, it is more difficult for P3PTT to be oxidized than P3PAT. The result indicates that P3PTT differs from P3PAT in terms of electron richness and the size of π-conjugated systems**.** From the onset oxidation potentials, we calculate out the highest occupied molecular orbital (HOMO) levels,[24] and then deduce the lowest unoccupied molecular orbital (LUMO) level from the HOMO and E_g data (Table 3). P3PTT has the HOMO level of 4.96 eV, lying below the HOMO level of 5.13 eV in P3PAT.

By measuring UV-vis-NIR spectra at different potentials, the electrochromic properties of P3PTT and P3PAT were investigated. The polymer films, which were prepared by spin coating on ITO glass, are electrochemically cycled in n-Bu_4NPF_6/MeCN electrolyte. As shown in Figure 5a, the P3PTT film at 0 V is pale yellow in color and exhibits strong absorption at 385 nm. In response to the oxidation, the absorption peak at 385 nm which is assigned to the π-π* transition declines while new absorption peaks appear at 315 nm, 512 nm，654nm, 782 nm and 885 nm, respectively. The peaks in the region of visible light are found to gradually increase. As a result, the P3PTT film changes in colour from yellow to brownish red. Figure 5b shows the optical transmittance of P3PTT film which is applied by the potentials from 0.6 V to 1.0 V vs Ag/AgCl. From the data in these curves, we calculate that optical transmittance change (ΔT) is 50% at 315 nm and 59% at 512 nm.

The neutral P3PAT film is yellow in color and exhibits strong absorption at 350 nm, as shown in Figure 6a. In response to the oxidation, the absorption peak at 350 nm declines while new absorption peaks appear at 450 nm, 631nm and 780 nm, respectively. It is found that during the oxidation process, the three peaks in the visible region are varied in unusual way, and the conventional monotonous tendency, which happens for P3PTT film, does not occur. From the 3D transmittance spectra in Figure 6b, we clearly observe that the intensity of the peak at 631 nm increases until 0.95 V, and the peak at 780 nm newly appears at this potential and increases with potential increasing. As a result, the colour of P3PAT film turns from a pale yellow to claybank till 0.95 V, followed by turning dark green with potential increasing. From the data in those curves, we obtain that the P3PAT film exhibits high optical contrast with ΔT of 77% at

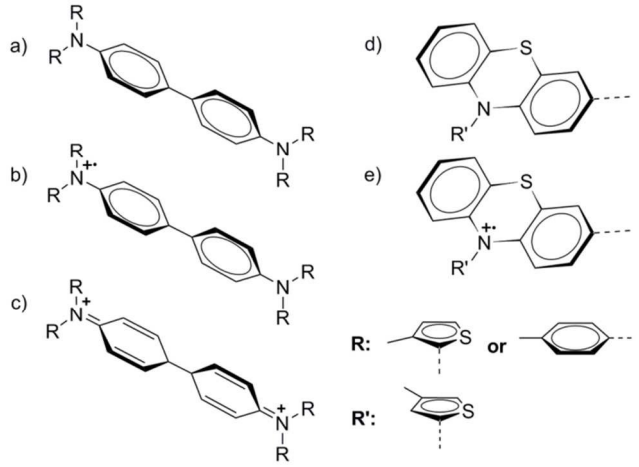

Fig. 8 The structural diagram of P3PAT in (a) neutral, (b) radical cation and (c) dication states. The structural diagram of P3PTT in (d) neutral and (e) radical cation states.

631 nm and 84% at 780 nm.

The potential step absorptometry was used to evaluate the polymer films in respect to coloration efficiency and switching properties. The absorbance change of the films was measured by stepping potential between the neutral state and oxidation state within a cycle time of 20 s. The amount of extracted/injected charge (Q) was calculated from integrating current density and time. The coloration efficiency (η) is calculate through the equation, $\eta = \delta OD/Q = \log [T_b/T_c]/Q$ where δOD is the change in optical absorbance at a specific wavelength and Q is the injected charge within continuous switching steps (Table S1). From the data in Figure 7, it is obtain that the coloration efficiency of P3PAT was as high as 201 cm^2/C at 780 nm. The high coloration efficiency is stabilized within 50 cycles. As for the P3PTT film, the coloration efficiency is 142 cm^2/C at 512 nm and has lower decay after continuous switching steps.

Previously, phenothiazine and its radical cations have been studied about the spectral absorption. The visible spectrum of phenothiazine solution reveal that the prominent peak at 512 nm increase largely after irradiation with ultraviolet light, which is accompanied with three absorbance peak increasing in the 600-900 nm.[25] The character of the spectrum did not change, and the intensity increase with the time of irradiation. It has been shown in figure 5a that absorption at 512 nm, 654 nm, 782 nm and 885 nm can only be observed in the oxidized state of P3PTT. As described above, phenothiazine in P3PTT here should be oxidized with a formation of radical cations as illustrated by the structure formula in Figure 8. In the UV-vis spectra of the oxidized P3PAT, the absorption peak at 780 nm is detected. This peak indicates that aromatic amine dication is produced[26]. In general, the dication originates from the further oxidation of radical cation. Two-stage oxidization is thus considered to occur in P3PAT film, as shown in Figure 8. The peak of the dication at 780 nm does not appear until 0.95 V. It is possible that the oxidation of the radical cation into dication commences at this voltage. With the above discussion, we ascribe the colouration from yellow to claybank as the first stage (0-0.95 V), from neutral to radical cation. The colouration from claybank to dark green is assigned to the second stage (0.95-1.25 V).

Conclusions

We have demonstrated the approach for synthesizing poly (3-(N, N-diphenylamino) thiophene) and poly (3-(10H-phenothiazin-10-yl) thiophene) through oxidation coupling reaction using $FeCl_3$ as oxidant. The as-synthesized polymers are soluble in the organic solvents and own good thermal stability at either nitrogen or air atmosphere. The fine structures of the synthesized two polymers were presented. The NMR spectral results revealed that the thiophene ring in 3PAT exhibit distinct reactive sites from the thiophene ring in 3PTT. The coupling reactions in the thiophene rings occurred at C1 atom for 3PAT and C2 atom for 3PTT. We have measured the electrochromic characteristics of the solution-cast polymer films. P3PAT exhibited high optical contrast in the visible/ near-infrared region, 84% at wavelength of 780 nm. P3PTT displayed the maximum optical contrast at 512 nm in the spectroelectrochemistry curves.

Acknowledgements

This work is supported by the Science and Technology Commission of Shanghai Municipality (STCSM) under grant no. 13DZ1108904.

Notes and References

[a] State Key Laboratory of Molecular Engineering of Polymer, Department of Macromolecular Science, Fudan University, Shanghai, 200433, The People's Republic of China, E-mail: xyni@fudan.edu.cn

† Electronic supplementary information (ESI) available. See DOI:
10.1039/b000000x

1 M. Redecker, D. D. C. Bradley, M. Inbasekaran, W. W. Wu and E. P. Woo, *Adv. Mater*., 1999, **11**, 241-246.
2 C. Li, H. Bai and G. Q. Shi, *Chem. Soc. Rev*., 2009, **38**, 2397-2409.
3 A. Choukourov, J. Hanuš, J. Kousal, A. Grinevich, Y. Pihosh, D. Slavínská and H. Biederman, *Vacuum.*, 2006, **80**,923-929.
4 M. Thelakkat, *Macromol. Mater. Eng*., 2002, **287**, 442-461.
5 L. Groenendaal, F. Jonas, D. Freitag, H. Pielartzik and J. R. Reynolds, *Adv. Mater*., 2000, **12**, 481-494.
6 G. Greczynski, Th. Kuglerb, M. Keila, W. Osikowicza, M. Fahlmanc and W. R. Salanecka, *J. Electron. Spectrosc. Relat. Phenom.,*2001, **121**, 1-17.
7 H. J. Yen and G. S. Liou, *Polym. Chem*., 2012, **3**, 255-264.
8 P. M. Beaujuge and J. R. Reynolds, *Chem. Rev.,* 2010, ***110,*** 268-320.
9 C. L. Ramírez and A. R. Parise, *Org. Electron.*, 2009,**10**, 747-752.
10 C. H. Yang, H. L. Chen, C. P. Chen, S. H. Liao, H. A. Hsiao, Y. Y. Chuang, H. S. Hsu, T. L. Wang, Y. T. Shieh, L. Y. Lin and Y. C. Tsai, *J. Electroanal. Chem*., 2009, **631**, 43-51.
11 K. R. Lin, Y. H. C. Chien, C. C. Chang, K. H. Hsieh and M. K. Leung, *Macromolecules.,* 2008, **41**, 4158-4164.
12 M. W. Thesen, B.Höfer, M. Debeaux, S. Janietz, A. Wedel, A. Kö hler, H. H. Johannes and H. Krueger, *J. Polym. Sci., Part A: Polym. Chem.,* 2010, **48**, 3417-3430.
13 M. Nagamochi, Y. Q. Fang and M. Lautens. *Org. Lett.,* 2007, 9,2955-2958.
14 H.Y. Lin and G.S. Liou, *J. Polym. Sci., Part A: Polym. Chem.,* 2009, **47**, 285-294.
15 M. Sun, J. Li, B. S. Li, Y. Q. Fu and Z. S. Bo, *Macromolecules.,* 2005, **38**, 2651-2658.
16 J. T. Kearns and M. E. Roberts, *J. Mater. Chem*., 2012, **22**, 2392-2394.

17 M. Watanabe, T. Yamamoto and M. Nishiyama, *Chem. Commun*., 2000, 133-134.
18 S. Hayashi and T. Koizumi, *Polym. Chem*., 2012, **3**, 613-616.
19 G. D. Sharma, M. Singh, R. Kurchania, E. N. Koukarascd and J. A. Mikroyannidis, *RSC Adv*., 2013, **3**, 18821-18834.
20 Y. Hiraiz and Y. Uozumi, *Chem. Commun*., 2010, **46**, 1103-1105.
21 J. McNulty, S. Cheekoori, T. P. Bender and J. A. Coggan, *Eur. J. Org. Chem.,* 2007, **9**, 1423-1428.
22 Y. Monguchi, K. Kitamoto, T. Ikawa, T. Maegawa and H. Sajikia, *Adv. Synth. Catal.,* 2008, **350**, 2767-2777.
23 X. X. Kong, A. P. Kulkarni and S. A. Jenekhe, *Macromolecules.,* 2003, ***36,*** 8992-8999.
24 H. J. Shine and E. E. Mach, *J. Org. Chem*., 1965, **30**, 2130-2139.
25 D. Sun, S. V. Rosokha and J. K. Kochi, *J. Am. Chem. Soc*., 2004, **126**, 1388-1401.
26 L. T. Huang, H. J. Yen and G. S. Liou, *Macromolecules*., 2011, **44**, 9595–9610.